

# Supporting Information

## Adhesion of Microdroplets on Water-Repellent Surfaces towards Prevention of Surface Fouling and Pathogen Spreading by Respiratory Droplets

*Jieke Jiang<sup>1,2</sup>, Hengdi Zhang<sup>1</sup>, Wenqing He<sup>1</sup>, Tianzhong Li<sup>1</sup>, Hualin Li<sup>1</sup>, Peng Liu<sup>1</sup>, Meijin Liu<sup>1</sup>, Zhaoyue Wang<sup>1</sup>, Zuankai Wang<sup>3</sup>, Xi Yao<sup>1\*</sup>*

<sup>1</sup>Department of Biomedical Sciences, City University of Hong Kong, Tat Chee Avenue, Kowloon, Hong Kong

<sup>2</sup>School of Veterinary Medicine, City University of Hong Kong, Tat Chee Avenue, Kowloon, Hong Kong

<sup>3</sup>Department of Mechanical and Biomedical Engineering, City University of Hong Kong, 83 Tat Chee Avenue, Kowloon, Hong Kong, P. R. China

\*Corresponding authors: xi.yao@cityu.edu.hk

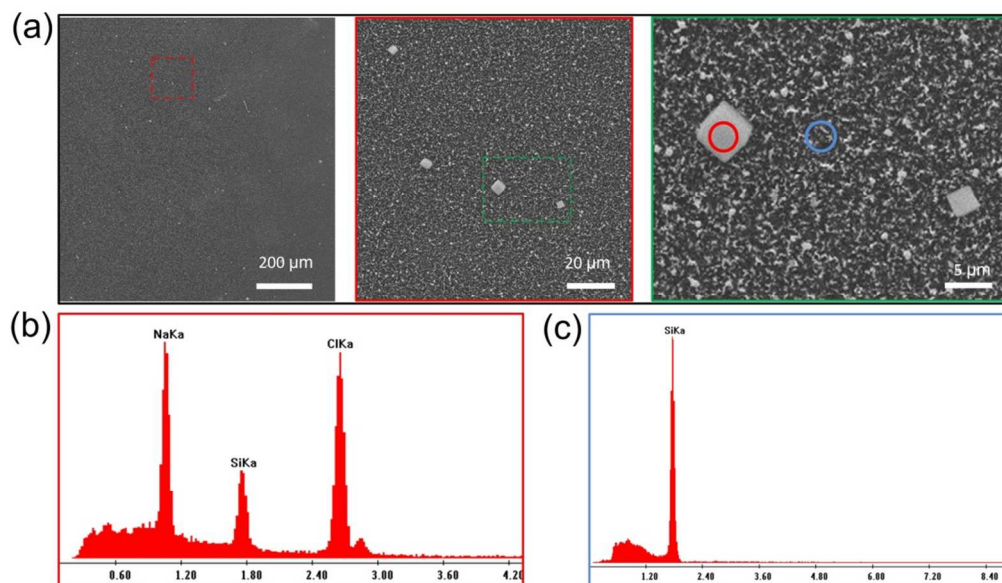


**Figure S1.** (a) SEM images of cubic NaCl crystals collected on the SH substrate after the evaporation of the sprayed microdroplets. The NaCl crystals are used to calculate the diameter of sprayed droplets. (b) Energy dispersive X-ray spectroscopy (EDS) element analysis of the collected cube, indicating the cube is composed with NaCl. (c) EDS element analysis of the background, which is composed with silicon and there is no signal of Na and Cl.

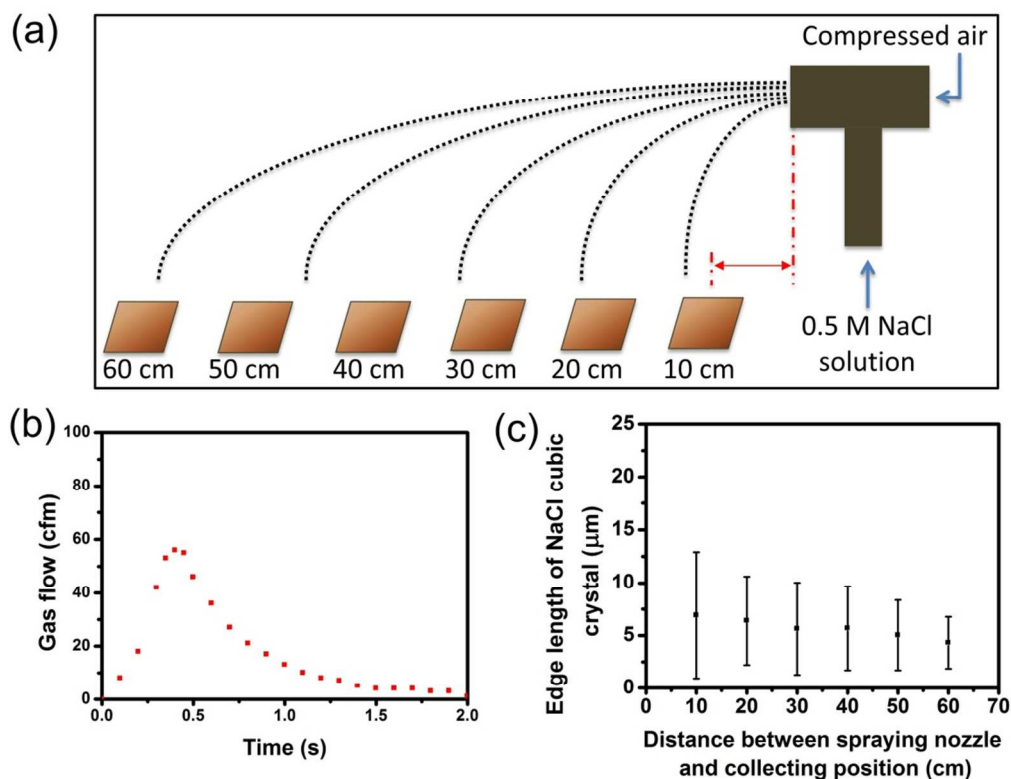


**Figure S2.** (a) Scheme showing the facility used to generate microdroplets with controlled diameter. (b) The gas flow of the compressed air applied to the sprayer. (c) Average length of cubic NaCl crystals collecting at different distances to the nozzle of the sprayer. The edge length of the crystals decreased as the collecting distance increased. The standard deviation of the edge length also decreased, since only small microdroplets travel a long distance.

## Calculation of parameters of SH surface

The height of the pillars ( $H$ ) was calculated based on 30 measurements. The pitch ( $p$ ) and diameter ( $d$ ) of pillars were calculated based on 100 measurements. The meanings of parameter  $p$ ,  $d$  and  $L$  are illustrated in Figure S3. The roughness and solid fraction of the SH surface can be expressed as  $\Phi_s = \frac{\pi d^2}{4(L+d)^2}$  and  $R = \frac{\pi d H}{(L+w)^2}$ , respectively.

The pinning of droplet on the surface occurs when the maximum pressure difference ( $\Delta P_{\text{MAX}} = \frac{-4\gamma \cos \theta_a}{L}$ ) across the liquid–solid interface is small than the dynamic pressure of the droplet ( $P_d = \frac{1}{2}\rho v^2$ ), where  $\gamma$  is the surface tension of water,  $\theta_a$  is the advancing contact angle of the droplet,  $\rho$  and  $v$  are the density and velocity of the droplet.<sup>1</sup> We calculated the  $\Delta P_{\text{MAX}}$  of water droplet on the SH surface and  $P_d$  of microdroplets with different diameter.  $\Delta P_{\text{MAX}}$  is in the scale of  $10^5$  Pa while  $P_d$  is in the scale of  $10^2$  Pa. Based on the calculation, the microdroplet should not pinned on the SH surface. However, the silicon nanowires are randomly distributed on the surface, which is different from the above calculation. There are defects between the randomly distributed nanowires. If regularity of the silicon nanowires on the SH surface could be improved, it may repel microdroplet with much smaller diameters.

(1) Quere, D., Wetting and Roughness. In *Annual Review of Materials Research*, **2008**, pp 71-99.

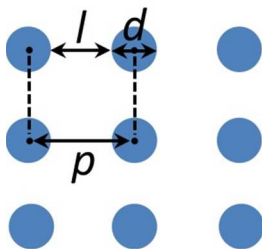


**Figure S3.** Schematic of the top view of the SH surface.

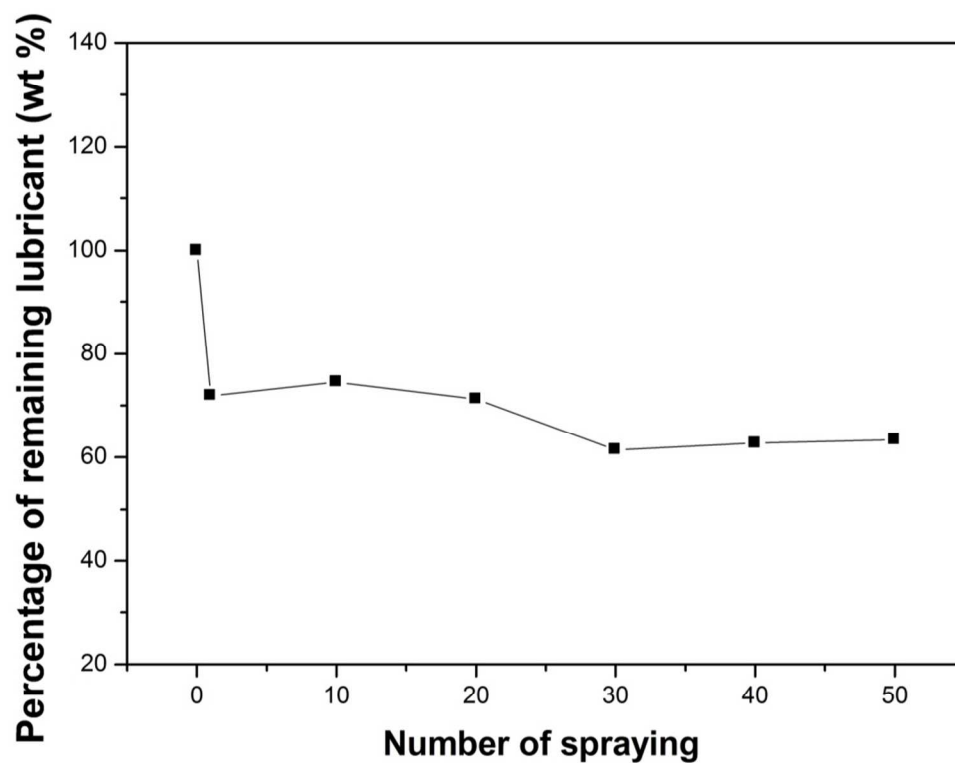


**Figure S4.** The percentage of remaining lubricant after different times of spraying. After the first spraying, almost 30% of lubricant was lost. After that, the loss of the lubricant decreased and the lubricant layer tend to be relatively stable.

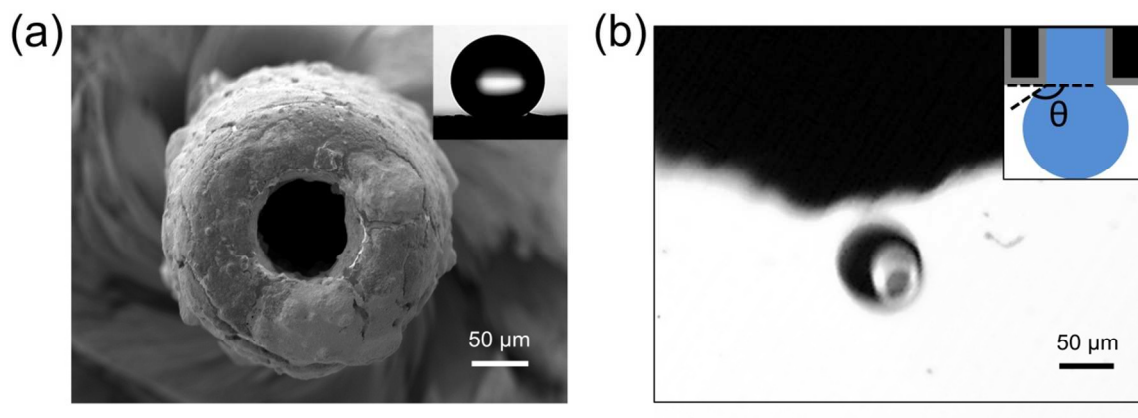


**Figure S5.** (a) SEM image of the superhydrophobic needle. Insert shows the contact angle of 5  $\mu\text{L}$  water droplet on the superhydrophobic coating used to fabricate the superhydrophobic needle. (b) Microscope image shows the generation of single microdroplet using the superhydrophobic needle. Insert scheme illustrates the generation process of single microdroplet.

**Table S1.** Retention Force and Gravity Force in tangential direction of Microdroplets on SH Surface and LIS surface

Superhydrophobic surface:

<b>Droplet Diameter (<math>\mu\text{m}</math>)</b>	<b>Receding Contact Angle <math>\theta_R</math></b>	<b>Advancing Contact Angle <math>\theta_A</math></b>	<b>Retention Force (<math>\mu\text{N}</math>)</b>	<b>Gravity Force (<math>\mu\text{N}</math>)</b>
40	145	148	0.000045526	0.000279296
60	145	147	0.000187078	0.000942624
75	144	149	0.000180052	0.001841063
85	147	150	0.000276828	0.002680042
290	163	164	0.004257122	0.106433609
750	164	168	0.070754243	1.841062729

LIS surface:

<b>Droplet Diameter (<math>\mu\text{m}</math>)</b>	<b>Receding Contact Angle <math>\theta_R</math></b>	<b>Advancing Contact Angle <math>\theta_A</math></b>	<b>Retention Force (<math>\mu\text{N}</math>)</b>	<b>Gravity Force (<math>\mu\text{N}</math>)</b>
40	49	52	0.000011	0.000279
60	89	90	0.000035	0.000943
90	55	56	0.000128	0.003181
250	83	84	0.001286	0.068188
350	85	86	0.002152	0.187107
750	110	111	0.014370	1.841063



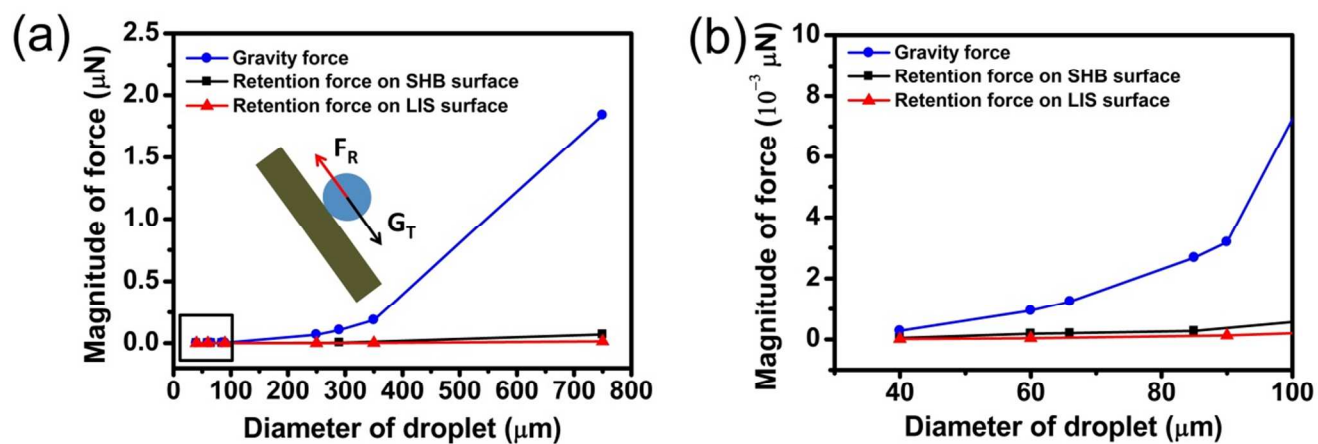


**Figure S6.** (a) Tangential gravity force and retention force of microdroplets on SH surface and LIS surface. (b) Zooming in of the force curves inside the black square in (a).

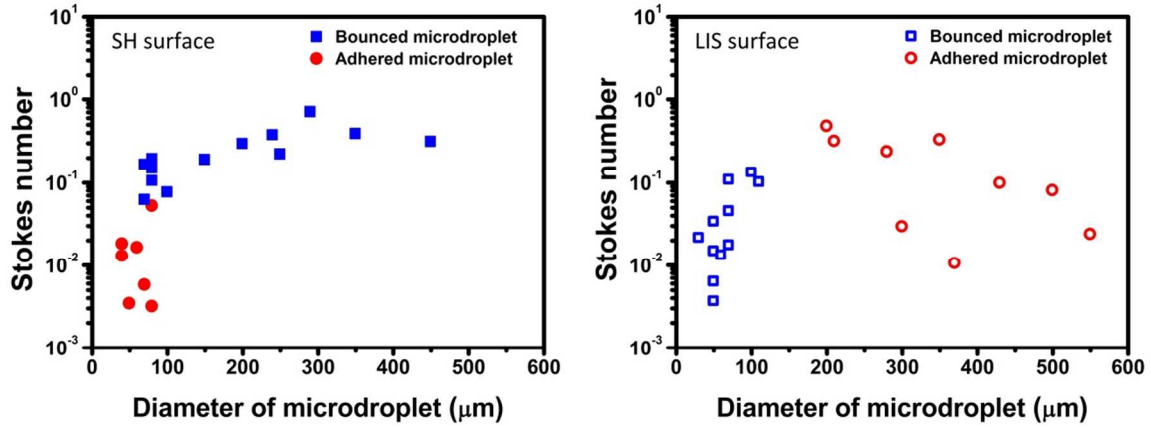


**Figure S7.** The Stokes number of microdroplets with different adhesion on the SH surface and LIS surface.

We estimated the Reynolds number of the microdroplets is in the range of 0.01-10. The deposition of the droplet is in Stokes regime. The Stokes number could be calculated by

$$Stk = tv/d$$

Where  $t$  is the relaxation time of the droplet,  $v$  is the velocity of the air flow,  $d$  is the diameter of droplet. At low Reynolds number,

$$t = \rho d / (18\mu)$$

where  $\rho$  is the density of air and  $\mu$  is the kinematic viscosity of air.

The Stokes number of those deposited droplets could be found in Figure S6. On the SH surface, the Stokes number of droplet greatly influence its adhesion. When the Stokes number is lower than 0.1, the droplet adhered on the surface. On the LIS surface, the Stokes number did not have predominant influence on its adhesion. Only larger droplet could slip off the LIS surface although the smaller droplet had the same Stokes number with the larger one.

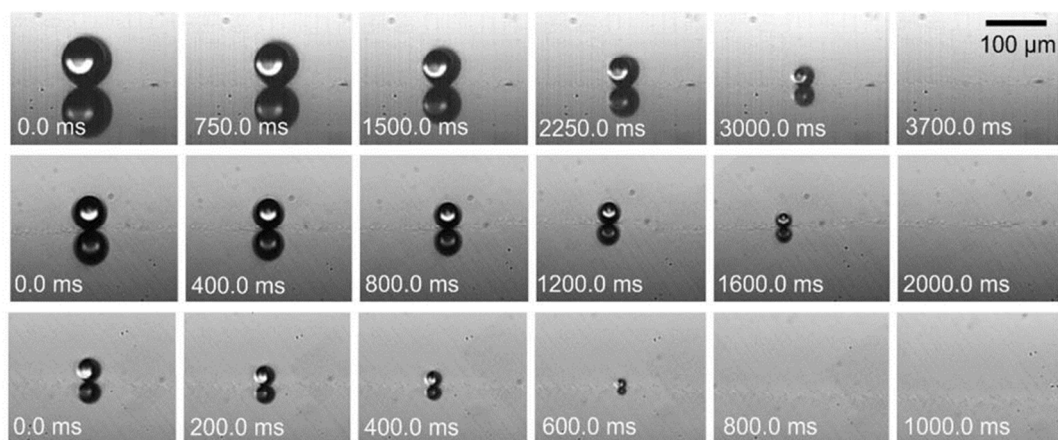


**Figure S8.** Time-dependent image sequences show the fast evaporation of microdroplets.

**Table S2.** Thickness of the lubricant layer calculated by weighting the LIS surface with and without the lubricant. The size of the sample is 76 mm x 25 mm. The lubricant layer was removed by wiping the sample with lens paper.

	<b>Sample Mass with lubricant (g)</b>	<b>Sample Mass without lubricant (g)</b>	<b>Mass of Lubricant (g)</b>	<b>Thickness of Lubricant (μm)</b>
Sample 1	6.0856	6.0722	0.0134	7.50
Sample 2	6.0991	6.0848	0.0143	8.00
Sample 3	6.9474	6.9329	0.0145	8.11
Sample 4	6.5599	6.5458	0.0141	7.89
Sample 5	6.1139	6.0986	0.0153	8.57
Average	6.36118	6.34686	0.01432	8.01

### The wrapping layer on LIS surface

The wrapping of droplet could be controlled by adjusting the surface tension of the lubricant.<sup>2</sup> The spreading of oil on the water droplet is determined by the coefficient  $Sow = \gamma_{wa} - \gamma_{wo} - \gamma_{oa}$ . If the  $Sow > 0$ , the oil will cloak the water droplet. The surface tension of the silicone oil here we use is ca. 20 mN/m and the water-oil interfacial tension is ca. 47 mN/m. The silicone oil will tend to cloak the water droplets. By increasing the oil-water interfacial tension, the LIS surface may perform much better in repelling microdroplets.

(2) Smith, J. D.; Dhiman, R.; Anand, S.; Reza-Garduno, E.; Cohen, R. E.; McKinley, G. H.; Varanasi, K. K. Droplet Mobility on Lubricant-Impregnated Surfaces. *Soft Matter* **2013**, 9, 1772-1780.

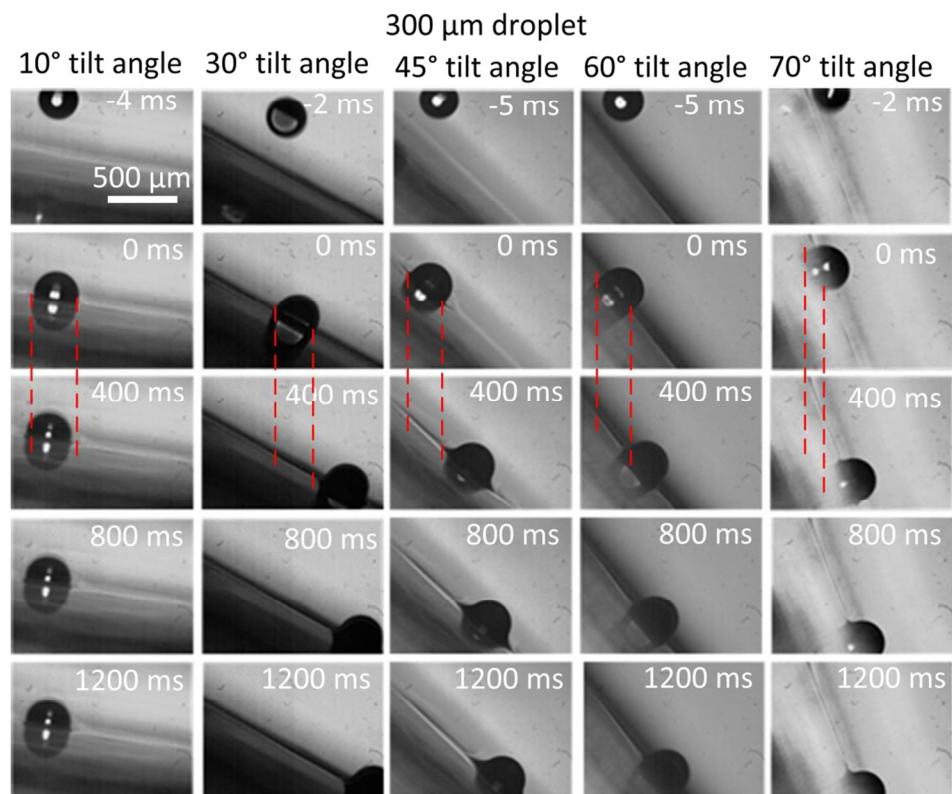


**Figure S9.** A 300  $\mu\text{m}$  microdroplet deposited on LIS surface with different titled angels.

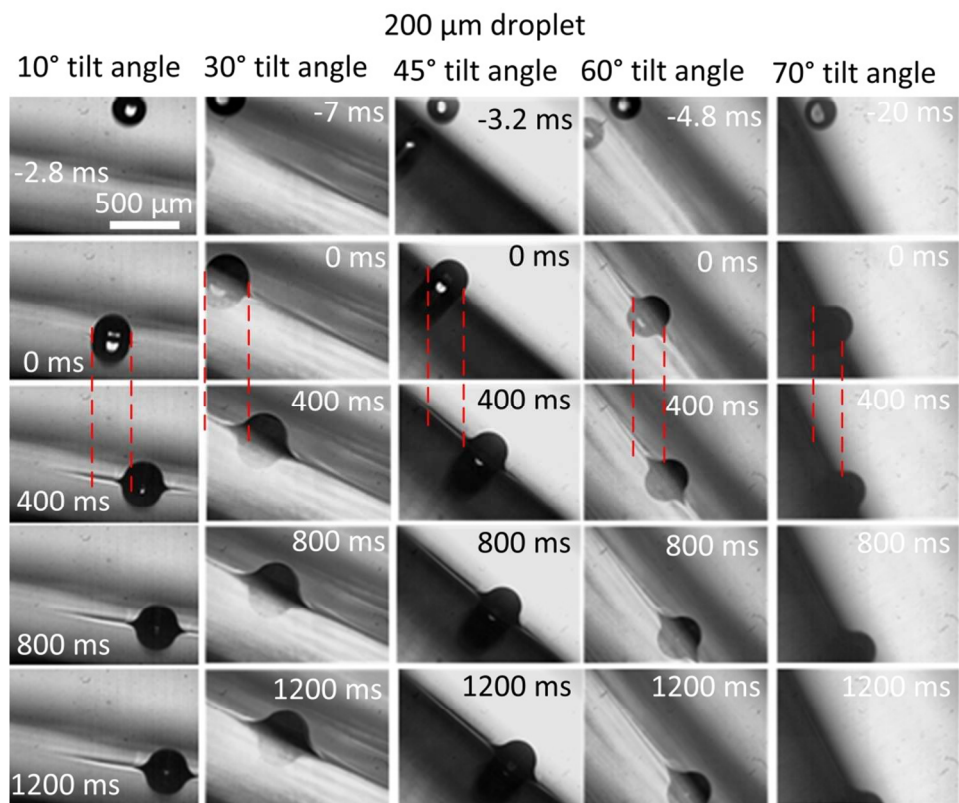


**Figure S10.** A 200  $\mu\text{m}$  microdroplet deposited on LIS surface with different tilted angles.

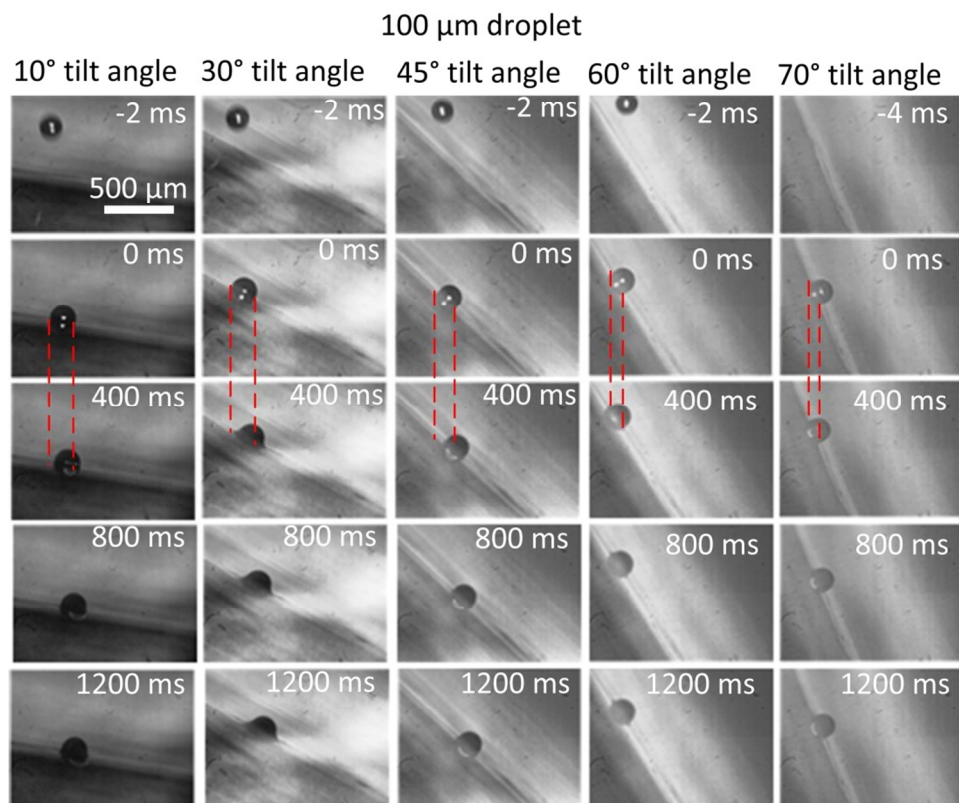


**Figure S11.** A 100  $\mu\text{m}$  microdroplet deposited on LIS surface with different titled angles.

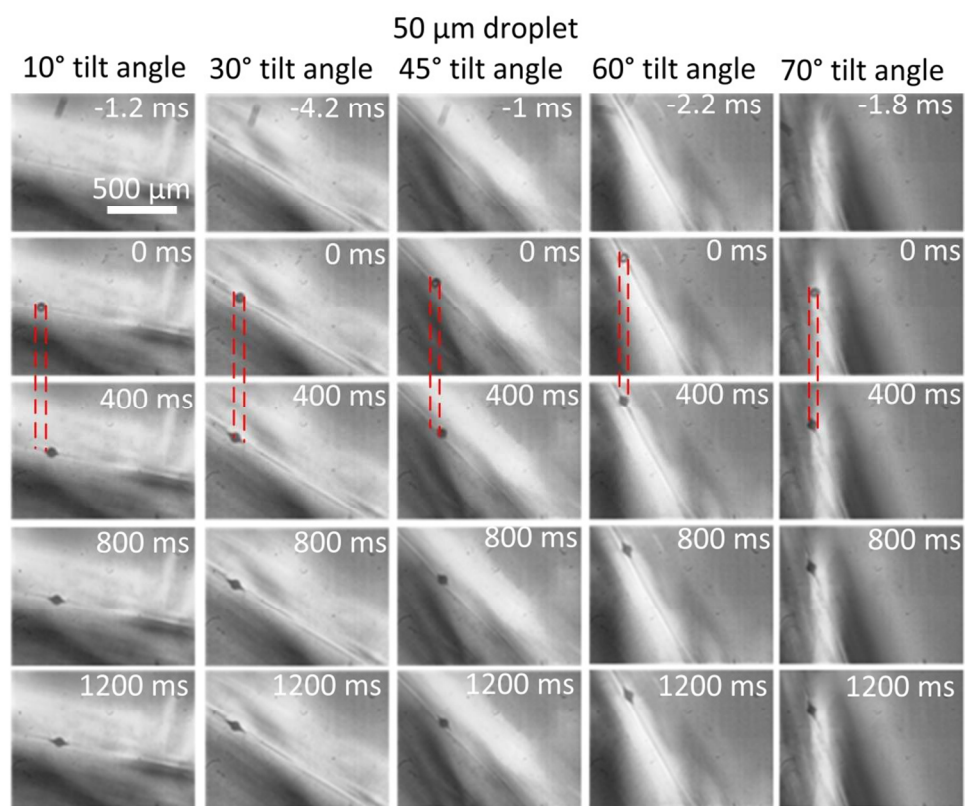


**Figure S12.** A 50  $\mu\text{m}$  microdroplet deposited on LIS surface with different titled angels.



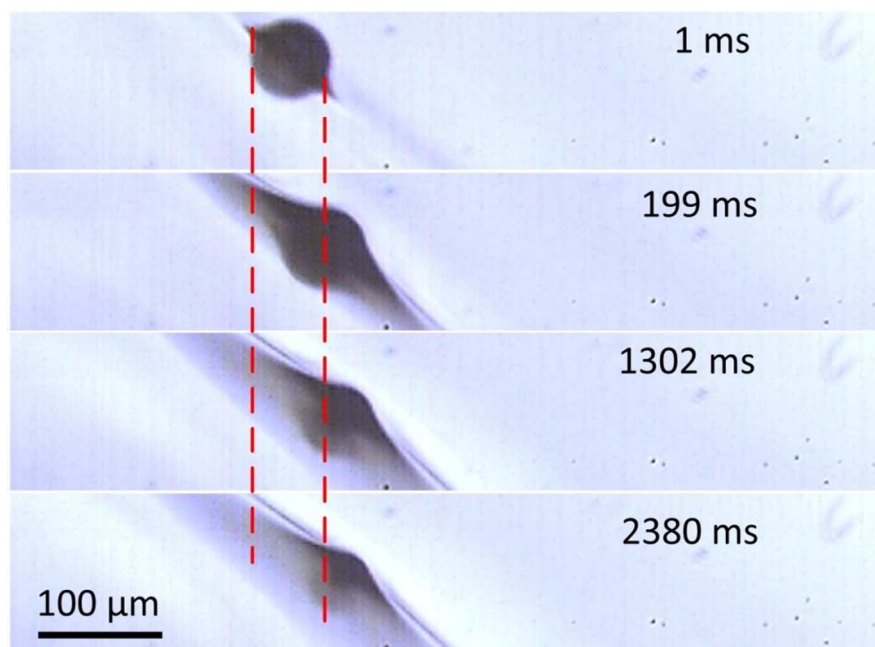


**Figure S13.** Microscope image sequences of a 40  $\mu\text{m}$  pinned on a 45° tilted LIS surface. After the 40  $\mu\text{m}$  microdroplet contact with the LIS surface, there is a very short mobile period before it was pinned.